Behaviour of laminar RC structures subjected to cyclic loading

Rajendra Varma

Indian Institute of Technology, Jammu, India

Joaquim Barros, Jose Sena Cruz

Universidade do Minho - Campus de Azurem, Portugal

Contacting author: rajendra.varma@iitjammu.ac.in

Abstract

When a concrete element is subjected to a multi-axial stress field, a suitable failure criterion is required to define the failure of concrete, e.g. Mohr-Columb, Drucker Prager, etc. This paper presents the modelling of laminar concrete structures like walls that can be considered as a plane stress problem, or 3D plane shells assumed as the assemblage of layers in plane stress state.

Some of the important aspects of the plane stress simulation are to address the following issues: the strength of concrete subjected to biaxial stresses; deviation in material properties before and after cracking; concrete cracking and, the crack propagation. As all these mechanical behaviours are critical to predict the behaviour of laminar structures, hence the issues are investigated by development of numerical model. Cyclic material constitutive laws were implemented in in-house finite element software – FEMIX. The material model matches the existing experimental evidence for the behaviour of reinforced concrete shear wall subjected to monotonic and cyclic loading. The implemented model does simulate the strength increase of concrete when submitted to biaxial compression, and the strength decrease when submitted to tension-compression and tension-tension, as was evidenced by experimental research.

Keywords: Concrete and Steel constitutive laws; Material modelling; Shells; Smeared Crack; Plane stress element

1. Introduction

Almost all reinforced concrete (RC) frames can be considered as a combination of beams, columns, shear-walls and slabs. In case of seismic analysis of multi-storey buildings, the approach followed that involves lumping of each storey at floors cannot predict the response of its sub-elements like beams and columns. In this case of multi-storey frame, beams, columns, beam-column joints and slabs need to be analysed independently for the purpose of detailing, as well as with other structural components inside a complete structure, for the overall response of structure to seismic loads. In the last decades researchers have proposed several ways of analysing these type of structures. The nonlinear finite element analysis (NLFEA) is one of the well accepted methods. By using computational tools of acceptable time consumption, the structural analysis problems which used to take very long time when using models of high sophistication, sometimes even

days, can now be solved in just a few minutes on personal computers.

The constitutive modelling of all the building materials is one of the key factors in achieving the goal to estimate the behaviour of structure accurately and reliably under repeated inelastic, varying and irregular load cycles. In some of constitutive models, huge number of iterations are required, which in turn evaluates the stresses from constitutive laws as their basic step, for NLFEA of large structures. When a concrete element is subjected to a multi-axial stress field, a suitable failure criterion is required to define the failure of concrete, e.g. Mohr-Columb, Drucker Prager, etc. The present work includes the modelling of laminar concrete structures like walls that can be considered as a plane stress problem, or 3D plane shells assumed as the assemblage of layers in plane stress state.

A biaxial model based on orthotropic nature of concrete is implemented in FEMIX under plane stress condition. The same model is also extended to laminar structures simulated by Mindlin Shell theory [1]. The purpose of implementation of these models in FEMIX is to analyse the whole class of structure which are in plane stress condition e.g. beams, and shear-walls, and then extend the formulation for shell structures that can be modelled by Reissner-Mindlin type shell finite elements.

The material model matches the existing experimental evidence for the behaviour of reinforced concrete under monotonic and cyclic loading. The model is simple to synthesize and yet robust to estimate the experimental behaviour with a satisfactory accuracy. The implemented model does simulate the strength increase of concrete when submitted to biaxial compression, and the strength decrease when submitted to tension-compression and tension-tension, as was evidenced by experimental research, and modelled by [3]. The tensile behaviour of the implemented model can simulate tension stiffening too.

2. Plane stress elements

The Reissner-Mindlin theory is one of the most widely used to estimate the behaviour of laminar structures. While both plane stress and Mindlin shell use the same type of finite elements, the laminar structures can be composed of several layers with distinct material characteristics. The behaviour of each layer is estimated independently for the membrane, bending and out-of-plane shear nonlinear behaviour. Several researchers ([3], [4]) have implemented the layered approach of laminar structures in finite element codes.

Figure 1 represents the basic features of Reissner-Mindlin shell decomposed in layers. Any generic layer is represented by k with its thickness as h_k along x_3-axis. The bottom, mid and top of the k^{th} layer is represented by $x^b_{3,k}$, $x^m_{3,k}$ and $x^t_{3,k}$, respectively. The height of the shell element is assumed to be h, which can vary along nodes. It is assumed that the degree of freedom (u_1 and u_2) of each node allows in plane deformation and, the stress in direction x_3 is negligible compared to the other stress components. The section normal to the middle surface of the shell may not remain perpendicular to the middle surface during deformation. This assumption is similar to the Timoshenko beam theory, where the plane sections perpendicular to the axis of beam need not be perpendicular to axis after deformation.

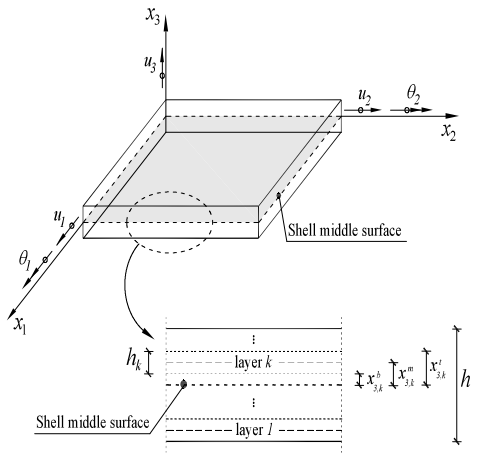

Figure 1. Multi-layer plane shell: displacements, rotations and k layer geometry definition (adapted from [1]).

When the 3D shell finite element (see Figure 1 and 2) is divided into layers through the thickness, the layers can be assumed of distinct thickness and

material properties. The constitutive stress-strain relation of each layer is applied at middle surface of that layer. As the in-plane strains along the thickness of the shell does not remain same as the middle surface, the strain in each layer differs, so does the stress state. Hence the contribution of stress and stiffness of each layer varies; depending on the position from the mid-surface, even if the material characteristics of different layers may be same.

Constitutive relation described in [5] is implemented at the finite element sampling point level for the calculation of internal equivalent nodal forces and stiffness. The algorithm followed for the calculation of stiffness matrix and internal equivalent nodal forces for element level from its constituent layers is described in Figure 3. Once the displacement field at finite nodes is known, using shape functions it is converted to displacement ($\underline{a}$) at the sampling points. The strains ($\underline{\varepsilon}$) are calculated at the mid-surface of each layer by derivative operators. Once the strains are calculated at sampling point of each layer, the tangent constitutive matrix or corresponding stresses can be calculated by constitutive relation of the material for each layer. The calculated quantities are then assembled at finite element level for tangent stiffness matrix ($\underline{K}_T^e$) or internal equivalent nodal force vector ($\underline{f}_{\text{int}}^e$). Figure 2 illustrates schematically the calculation procedure of internal forces.

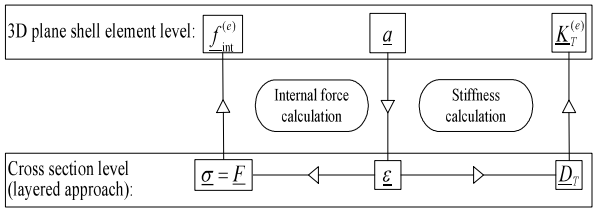

Figure 2. Scheme to obtain the tangent stiffness matrix and internal equivalent nodal forces of an element.

3. Smeared crack model

Both the approaches, discrete as well as smeared, have their advantages and disadvantages. In case when there are very few cracks that govern the response of structure, the discrete crack approach is the possible option, but in case when the reinforcement is dense or a strain hardening cement material is used, diffuse crack patterns can be formed, which is favourable to the use of a smeared crack approach (see Figure 4(a)).

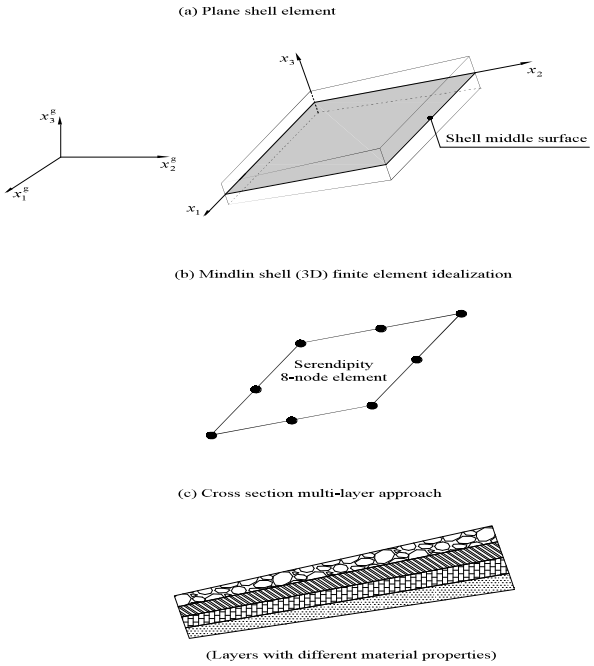

Figure 3. Example of a finite element idealization of a plane shell element according to the multi-layer (adapted from [1]).

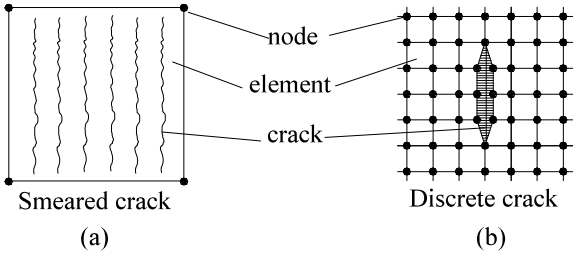

Figure 4. (a) Smeared and (b) discrete crack formed by nodal separation on element boundaries.

The smeared crack approach is more popular also due to three reasons:

- The crack is allowed to form in any direction;
- When the overall behaviour of the structure is important compared to the localized zones;

- During the calculation, only the stiffness matrix at integration point is changed compared to the finite element topology.

The smeared crack approach can be divided in two categories: a) fixed and b) rotating crack. As soon as the maximum tensile stress at any integration point reaches the peak tensile strength for the first time, a crack is introduced at that point. The material behaviour at that point in the direction parallel to the crack and orthogonal to it, can be treated differently based on stress state induced anisotropy, directionally dependent, as opposed to isotropy [7, 8]. It is to be noted that at the instant of crack formation, the direction of principal stress coincides with the direction of principal strain. The crack can be assumed in local coordinate system (hereafter crack coordinate system), defined by ***ns***-coordinate system, where ***n*** and ***s***-axes represent the direction normal and tangential to crack, respectively. In fixed crack approach, the direction of ***n***-axis (normal to the crack) is fixed, as one of the orthotropic direction for the rest of analysis/response. This permanent allocation of damage is the main characteristic of fixed crack approach. During subsequent loading the ***n*** and ***s*** coordinate axis may not remain the new principal directions of stress and strain. If a new principal stress is calculated, then it may exceed the tensile strength, and should be a criterion for another crack.

But as the direction of ***n*** and ***s*** axes are fixed and the condition of cracking is checked for only ***s***-direction and not any direction in between these axes. Hence, a new crack can form only in the ***n***-direction. This approach yields to stiffer response, and can be avoided by assuming non-orthogonal cracks. [9] proposed a strategy, in which, if the angle between previously calculated principal stress and newly calculated principal stress exceeds the empirically defined threshold angle, then a new crack is recorded. The non-orthogonal fixed crack approach has been investigated, but it assumed no threshold angle concept, which is found to have no discontinuity as reported by various researchers. These models assume either secant or elastic unloading. Some algorithms retain the crack closing in memory, while some assume the crack to become inactive and new cracks are formed. Moreover it is to be noted that the fracture energy [6] available to new cracks keeps decreasing as some part of it is utilized in the previous cracks formed at that gauss point.

It has been reported that rotating crack approach produces less stiff response than the non-orthogonal fixed crack model [7, 8]. However, smeared crack approach has a drawback of stress-locking in the vicinity of dominant discrete crack, still it is less severe in case of rotating crack approach. In smeared crack approach, when a crack is formed in any element, it results in softening of that element; if further strain increment happens for that element, because of displacement continuity, the neighbouring un-cracked element are forced to follow it, a spurious increase in the stress of un-cracked element is observed. This is contrary to the strain localization and undesirable.

4. Material non linear models

4.1 Genesis of biaxial concrete constitutive laws

The concrete can be assumed to follow linear elastic isotropic behaviour until cracking. In global ***xy*** coordinate system, based on the total strain approach, the constitutive relationship is described as:

$$\underline{\sigma}_{xy} = \underline{D}_{xy}\underline{\varepsilon}_{xy} \tag{1}$$

$$\begin{bmatrix}\sigma_x\\ \sigma_y\\ \sigma_{xy}\end{bmatrix} = \frac{E}{1-\nu^2}\begin{bmatrix}1 & \nu & 0\\ \nu & 1 & 0\\ 0 & 0 & (1-\nu)/2\end{bmatrix}\begin{bmatrix}\varepsilon_x\\ \varepsilon_y\\ \gamma_{xy}\end{bmatrix} \tag{2}$$

where *E* and ν are the elasticity modulus and the Poisson's ratio of concrete, respectively; σ_x and σ_y are normal stresses in ***x*** and ***y*** direction, and ε_x and ε_y are the corresponding normal strains; τ_{xy} is the shear stress in ***xy*** plane corresponding to shear strain γ_{xy}.

Once the concrete is cracked, it can be assumed to follow orthotropic behaviour. The direction of orthotropy can coincide with the direction of principal stresses.

Assuming that the stresses are not coupled in the crack local coordinate system, Eq. (1,2) will be replaced by:

$$\underline{\sigma}_{ns} = \underline{D}_{ns}\underline{\varepsilon}_{ns} \tag{3}$$

$$\begin{bmatrix}\sigma_n\\ \sigma_s\\ \tau_{ns}\end{bmatrix} = \begin{bmatrix}E_n & 0 & 0\\ 0 & E_s & 0\\ 0 & 0 & G_{ns}\end{bmatrix}\begin{bmatrix}\varepsilon_n\\ \varepsilon_s\\ \gamma_{ns}\end{bmatrix} \tag{4}$$

where σ_n and σ_s are normal stresses corresponding to ε_n and ε_s, respectively; τ_{ns} is the shear stress corresponding to γ_{ns}, shear strain in ***ns*** plane; E_n and E_s are tangential moduli in ***n*** and ***s*** direction, respectively, while G_{ns} is the shear modulus in ***ns*** plane. It is to be noted that the local shear stress component τ_{ns} of the stress vector $\underline{\sigma}_{ns}$ is always zero according to the definition of the rotating crack model.

One of the important assumptions in the formulation is based on realistic condition is that the principal strain (ε_i) at any sampling point in *i*-direction (*i*=*n, s*) is the sum of an elastic (ε_i^{el}) and a cracked concrete (ε_i^{cr}) component. The assumptions of the modifications are: principal strains are assumed independent to each other in calculation; only elastic part of principal strain is used to calculate the Poisson's effect, for one direction to other direction of ***ns*** co-ordinate system.

$$\varepsilon_i = \varepsilon_i^{el} + \varepsilon_i^{cr} \tag{5}$$

The Eq. 5 can be modified to take into account this effect as:

$$\begin{bmatrix}\varepsilon_n^*\\ \varepsilon_s^*\end{bmatrix} = \frac{1}{1-\nu^2}\begin{bmatrix}1 & \nu\\ \nu & 1\end{bmatrix}\begin{bmatrix}\varepsilon_n^{el}\\ \varepsilon_s^{el}\end{bmatrix} + \begin{bmatrix}\varepsilon_n^{cr}\\ \varepsilon_s^{cr}\end{bmatrix} \tag{6}$$

4.2 Concrete constitutive model

The uniaxial model of concrete in compression and hysteretic scheme (compression and tension both) described in [5] is used for ***ns*** directions, while only tension envelope is assumed to be a tri-linear curve as it is different from the one described in [5]; however the entities will be in similar format.

4.3 Modelling of steel

The steel reinforcement can be modelled in three ways, namely, smeared reinforcement, embedded cable and discrete steel models. FEMIX already has two types of models, embedded cable and discrete cable element. The smeared reinforcement model was implemented in FEMIX, under the framework of laminar structures.

5. Model appraisal for cyclic loading

5.1 Cyclic loading test

To validate the cyclic laws a barbell-shaped shear wall B2, which was tested by [10] at the Portland Cement Association, was used for the numerical analysis. The isolated shear wall B2 (hereafter shear wall) was approximately 1/3-scale models of full size walls, and was composed of wall web and boundary elements (see Figure 5(a), Figure 6), which were sandwiched between stiff base block and stiff top slab. The wall was tested like a vertical cantilever with reversing horizontal displacements applied through the top slab. The boundary element was 4570 mm (high) × 305 mm (long) × 305 mm (thick) and the vertical reinforcement in it amounted to 3.67% ($12\,\phi\,20$). The wall web was 4570 mm (high) × 1910 mm (long) × 102 mm (thick), and was reinforced with 0.28% ($12\,\phi\,6$) in the vertical direction. The horizontal reinforcement of $\phi\,6$ was placed uniformly throughout the wall web at 203 mm distance and, was extended inside the boundary elements. In boundary elements the horizontal ties (see Figure 5(b), Figure 6) were placed simultaneously with web ties.

The stiff top slab of shear wall was subjected to cyclic horizontal displacement as illustrated in Figure 7(a), where every displacement cycle was repeated two times, before the extreme displacement of the next cycle was incremented by 25 mm in each direction.

The shear wall can be divided in three zones to reflect the change in cross section and discretizing in mesh, namely side walls, wall web and top slab. The side walls were divided in 40, the wall web in 200 and the top slab in 18 four-node quadrilateral elements, of uniform shape in their respective zone (see Figure 5(b)). All the elements were discretized in 11 layers, namely layer pattern. All the zones followed the same layer pattern. Each element can be considered to be composed of three layers of steel (two horizontal and one vertical), two concrete cover layers and six layers of confined concrete. For the concrete cover and confined concrete it was assumed the same constitutive model, and the properties of the concrete are represented in Table 1. The steel bars were modelled smeared in this analysis and the properties of horizontal and longitudinal steel reinforcement are described according to the rebar type in Table 2. The concrete tensile properties were derived according to [2], however the compressive properties of concrete and mechanical properties of steel reinforcement is derived from [10]. All the layers assumed 2×2 Gauss-Legendre integration scheme for the Mindlin shell element in the calculation of the stiffness matrix and internal equivalent nodal forces. The displacements of the side wall and wall web were constraint at bottom to replicate the displacement of base block.

Table 1. Data used in constitutive model of concrete for simulation of shear wall B2.

Poisson's ratio, ν	0.2
Initial Young Modulus, E_c (GPa)	32.7
Peak compressive strength of concrete, f_{cc} (MPa)	53.7
Strain at peak compressive strength of concrete, ε_{cc} (mm/mm)	2.5×10^{-3}
Non-dimensional critical strain on the compression envelope, $\bar{\varepsilon}_{ccr}$ (mm/mm)	2.55×10^{-3}
Peak tensile strength, f_{ct} (MPa)	4.29
Strain at peak tensile strength, ε_{ct} (mm/mm)	7.8×10^{-5}
Fracture energy, G_f (N/mm^2)	0.20
Ratio between the strain at the first post-peak point and ultimate strain, α_1	0.10
Ratio between the stress at the first post-peak point and peak tensile strength, β_1	0.65
Ratio between the strain at the second post-peak point and ultimate strain, α_2	0.45
Ratio between the stress at the first post-peak point and peak tensile strength (β_2)	0.26

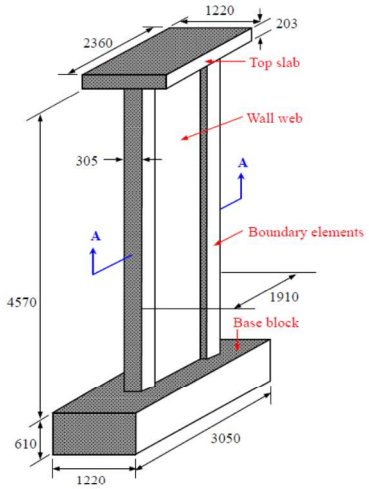

(a)

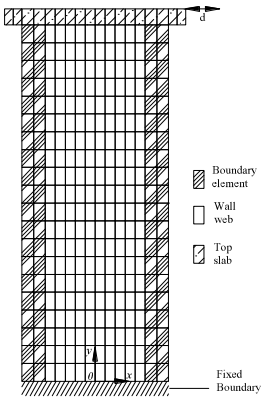

(b)

Figure 5. (a) Nominal dimension (adapted from He et al 2008) (b) Finite element mesh.

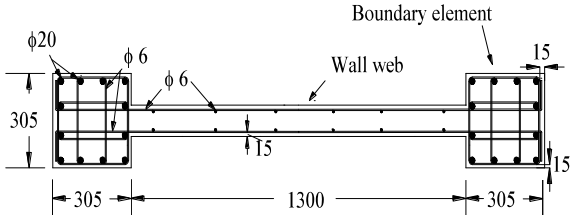

Figure 6. Cross-sectional details of shear-wall B2. Note: all units in millimetres.

Table 2. Data used in simulation of shear wall B2 for the behaviour of the smeared reinforcement.

Parameters	H^w, H^b, V^w	V^b
Initial Young Modulus, E_s (GPa)	200	200
Tangent modulus at strain hardening, E_{sh} (GPa)	6.4	6.4
Yielding strain, ε_{sy} (mm/mm)	2.7×10^{-3}	3.11×10^{-3}
Yielding stress, f_{sy} (MPa)	532.4	410.3
Hardening strain, ε_{sh} (mm/mm)	1.5×10^{-2}	1.5×10^{-2}
Hardening stress, f_{sh} (MPa)	544.0	425.0
Strain at the ultimate stress, ε_{su} (mm/mm)	1.68×10^{-2}	1.8×10^{-2}
Ultimate stress, f_{su} (MPa)	548.0	435

^{b} = Boundary element; ^{w} = Wall element, H = Horizontal reinforcement, V = vertical reinforcement.

The response obtained from FEMIX is compared with the experimental response and is illustrated in the Figure 7(b). The numerical response predicted satisfactorily the important characteristics of the cyclic loading, including the strength degradation in consecutive cycles, degradation of stiffness during reloading. The unloading path of simulated cycles closely follow the experimental path, while during reloading the experimental cycles predict lower stiffness in last few cycles. In the cycles with maximum displacement it was found that the concrete was almost crushed in compression, as also reported in experiment. The used numerical model did not allow neither bar buckling nor slip between concrete and steel. The bar-slip or buckling becomes almost certain in such cases, where the concrete cover is completely crushed or removed during loading. Researcher [10] has reported that the steel ties were visible in lower part of shear wall during last cycles, which led to ultimate failure of the shear wall. The experimental response show a high load carrying capacity, compared to numerical simulation. This might have caused due to slightly higher strength of the reinforcing bars in boundary elements compared to the tested specimen of reinforcing bars.

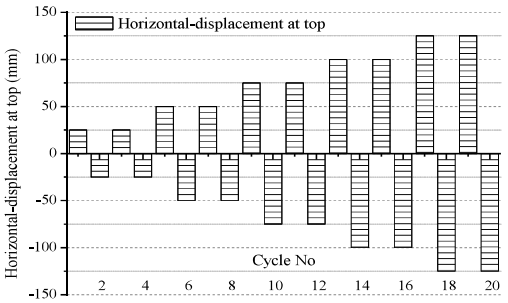

(a)

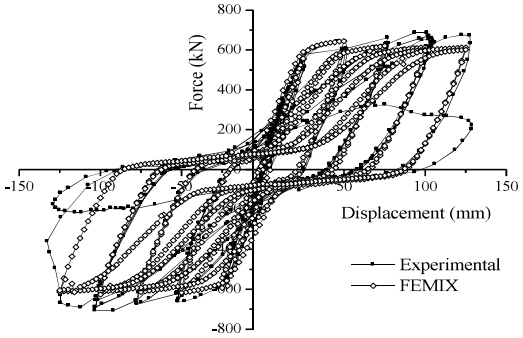

(b)

Figure 7. (a) Displacement loading history for shear wall B2 (b) comparison of Force versus

displacement graphs observed from experiment and estimated by FEMIX.

6. Summary

This paper describes a model developed for the analysis of reinforced concrete beams, shear-walls and plane shells that are submitted to monotonic and cyclic loads. For the same purpose, a biaxial constitutive model for concrete was implemented based on smeared crack approach. During post-cracking, the concrete model is based on condition that the effect of Poisson's ratio to other direction will cease as soon as the maximum strength condition is violated for this direction. However the elastic strain will still continue to contribute to other direction. The implemented model estimates the rotating smeared crack formation based on principal strain and principal stress. The principal stress and strain are assumed to be coaxial. Similarly, a steel model was also implemented to simulate smeared reinforcement. The implemented envelope curve for tension follows a tri-linear post-cracking behaviour, which can simulate the tension stiffening and softening depending on the fracture energy. The model is compared and validated with benchmark problems at material level and structural level by experimental results. The implemented model is able to predict the response of RC structures under hysteretic loading with acceptable accuracy.

7. References

[1] Ventura-Gouveia, A. Análise Experimental e Simulação Numérica de Elementos de Barra de Pórtico Tridimensional de Betão Armado (Experimental Analysis and Numerical Simulation of Reinforced Concrete 3D Frame Elements, MSc Thesis, Department of Civil Engineering, University of Minho, July [in Portuguese]; 2000.

[2] He, W., Wu, Y., and Liew, K. M. A fracture energy based constitutive model for the analysis of reinforced concrete structures under cyclic loading, *Computer Methods in Applied Mechanics and Engineering*, Oct, 2008, 197(51-52), 4745-4762.

[3] Huang, Hou-Cheng. Static and dynamic analyses of plates and shells – Theory, ISO TC 71/SC 6 *Non-conventional reinforcement of concrete-test methods-part 2: Fiber reinforced polymer (FRP) sheets*, International standard (2003).

[4] Barros, J.A.O. Modelos de análise de estruturas laminares e de compósitos laminados (Models for the analysis of laminar structures and laminate composites), MSc Thesis, Civil Eng. Dept., Faculty of Engineering, University of Porto, Portugal [in Portuguese]; 1989.

[5] Rajendra Varma. Numerical models for the simulation of the cyclic behaviour of RC structures incorporating new advanced materials, PhD Thesis, Department of Civil Engineering, University of Minho, March 2013.

[6] Barros, J.A.O. "Comportamento do betão reforçado com fibras. Análise experimental e simulação numérica. Behavior of fiber reinforced concrete. Experimental analysis and numerical simulation." PhD Thesis, Faculty of Engineering, University of Porto, Portugal. [in Portuguese]

[7] CEB 1996a. "RC elements under cyclic loading. state-of-art report." Comite Euro-Internaltional du Beton, Thomas Telford Publications, London; 1996.

[8] CEB 1996b. "RC frames under earthquake loading. state-of-art report." Comite Euro-Internaltional du Beton, Thomas Telford Publications, London.

[9] Rots, J.G., "*Computational modeling of concrete fracture*", PhD Thesis, Delft University of Technology; 1998.

[10] Oesterle, R.G., Fiorato, A.E., Johal, L.S., Carpenter, J.E., Russell, H.G., Corley, W.G. "Earthquake-resistant structural walls—Tests of isolated walls", Report to the National Science Foundation, Construction Technology Laboratories, Portland Cement Association, Skokie, Illinois, November, 315 pp.